PETROLOGY OF THE YAMATO-74191 CHONDRITE

Yukio IKEDA

Department of Earth Sciences, Ibaraki University, Mito 310

and

Hiroshi TAKEDA

Mineralogical Institute, Faculty of Science, University of Tokyo, Hongo 7-chome, Bunkyo-ku, Tokyo 113

Abstract: The chondrules in the Yamato-74191 meteorite (L3) are classified into seven groups by their SiO_2 contents and texture. The most common group (P III) shows intimate compositional relations between bulk composition of chondrules and olivines in them. The olivines in magnesian chondrules show wide compositional zoning from magnesian core to ferrous rim, whereas the olivines in ferrous chondrules are relatively homogeneous and have the same composition of ferrous rim olivines in the magnesian chondrules. This compositional relation may be explained by gradual increase and subsequent sudden decrease in the degree of oxidation state of silicate melt in the course of their crystallization.

1. Introduction

The Yamato-74191 meteorite is an unequilibrated chondrite found in the Yamato meterorites (YANAI *et al.*, 1978). On the basis of the bulk chemical composition, the sharply defined chondritic texture, and the presence of fresh glass, the 74191 chondrite is placed into the L3 group of VAN SCHUMUS and WOOD (1967).

Several types of chondrules have been known to occur commingled in a single chondrite (WOOD, 1968; VAN SCHUMUS, 1969), and the diversity in overall composition of these chondrules in terms of atom percentages of major elements has been estimated (WALTER, 1969). However, no detailed study of their chemical zoning trends of individual minerals has been undertaken. Since the least metamorphosed chondrites may carry more information of their crystallization and cooling history, we investigated about one hundred chondrules in Yamato-74191, by electron-probe microanalyzer, each chondrule being treated as a single rock specimen.

2. General Description

The bulk chemical composition of the Yamato-74191 chondrite is shown in Table 1. The Fe°/total Fe, total Fe/Si and Si/Mg of the chondrite are 0.5434, 0.4366 and 1.0806, respectively, where Fe° means irons present in metallic and/or sulfide phases.

Table 1. Chemical composition of the Yamato-74191 meteorite.

SiO_2	40.09	$H_2O(-)$	0.05
TiO_2	0.24	$H_2O(+)$	1.13
Al_2O_3	2.89	P_2O_5	0.20
FeO	14.68	FeS	5.01
MnO	0.35	Fe	5.66
MgO	24.89	Ni	0.85
CaO	1.79	Co	0.032
Na_2O	0.97	Cr_2O_3	0.75
K_2O	0.13	Total	99.712

Analyst: H. HARAMURA.

The chondrite consists of chondrules, mineral fragments and matrix. Here, matrix is defined to be aggregates of fine grained substances smaller than about 1 μm in size which fill interstices among chondrules and/or mineral fragments. Chondrules are defined as spherical or fragmented spherical substances which have textures of metallic, porphyritic, equigranular, barred-olivine, glassy (devitrified) or radial-pyroxene chondrule, which will be discussed in later sections. The volume of chondrules in the meteorite is more than 50%. Mineral fragments are substance larger than about 1 μm except chondrules. They are mainly olivine, pyroxene, opaque minerals and aggregates of these minerals.

3. Classification of Chondrules

3.1. Bulk chemical composition of chondrules

The bulk chemical composition of about fifty chondrules in the Yamato-74191 meteorite was analyzed by defocussed beam of electron-probe microanalyzer. The defocussed beam, the diameter of which is about 50 μm, is moved slowly on the polished surface of chondrules with manual method, and covers the nearly whole area of the chondrule in a fixed time of 20 seconds $\times$ 5 times, avoiding holes and large fractures in the chondrule. The correction method of the analyses is according to BENCE and ALBEE (1968), and the correction factors given by NAKAMURA and KUSHIRO (1970) were used. Although only negligible amounts of metallic and/or sulfide phases are generally observed in the chondrules, a few chondrules

Table 2. Chemical composition of chondrules in the Yamato-74191 chondrite.

Group of chondrule	P II			P III′							
Chondrule number	No. 40	No. 112	No. 101	No. 200	No. 14	No. 25	No. 2	No. 15	No. 165	No. 20	No. 164
SiO_2	36.36	38.89	39.11	39.29	38.14	41.45	41.96	40.62	42.70	42.62	42.35
Al_2O_3	3.78	5.57	5.53	2.22	4.48	2.90	2.73	2.96	3.52	5.59	3.27
MgO	28.17	33.39	34.22	36.47	29.61	29.12	30.68	30.64	26.40	33.70	27.50
ΣFeO	25.62	18.93	15.65	15.85	20.56	18.26	19.64	18.32	19.57	10.40	19.36
MnO	0.41	0.18	0.32	0.33	0.42	0.40	0.41	0.40	0.41	0.24	0.41
CaO	0.61	2.73	2.21	1.13	2.16	2.10	1.97	1.56	1.39	3.29	1.79
Na_2O	2.48	1.01	0.82	0.48	0.54	1.11	1.48	1.09	2.04	0.95	1.45
K_2O			0.03	0.00	0.03	0.92		0.67			
Cr_2O_3	0.77				0.99	0.51	0.62	0.56		0.32	
TiO_2			0.20	0.00	0.14	0.12		0.19			
NiO		1.18	0.22	0.15					1.17		0.26
Total	98.20	101.88	98.31	95.92	97.07	96.89	99.49	97.01	97.20	97.11	96.39

Group of chondrule	P III″											
Chondrule number	No. 36	No. 11	No. 16	No. 206	No. 24	No. 32	No. 205	No. 17	No. 4	No. 37	No. 26	No. 22
SiO_2	44.22	44.94	45.50	45.50	44.65	46.62	46.73	46.92	48.34	49.74	48.88	49.78
Al_2O_3	2.31	4.86	5.51	2.83	2.68	4.20	3.84	1.75	3.11	3.43	3.97	4.06
MgO	32.98	33.03	29.46	29.37	31.28	27.03	25.54	29.69	25.41	28.40	28.02	27.36
ΣFeO	17.51	14.16	12.52	15.38	12.47	15.72	15.12	13.71	16.25	11.25	11.38	9.08
MnO	0.46	0.17	0.48	0.53	0.42	0.47	0.43	0.48	0.44	0.47	0.36	0.49
CaO	1.55	1.13	3.40	1.90	1.57	2.12	2.37	2.21	2.67	2.22	1.53	2.41
Na_2O	0.03	1.87	1.08	1.77	1.47	2.27	1.89	1.05	1.70	2.26	1.22	1.22
K_2O			0.05					0.07				0.03
Cr_2O_3	1.01	0.38	0.92		0.79	0.77		0.98	0.71	0.73	1.17	0.82
TiO_2			0.18					0.11				0.20
NiO				0.23			0.06					
Total	100.07	100.54	99.10	97.51	95.33	99.20	95.98	96.97	98.63	98.50	96.53	95.45

Table 2 (Continued).

Group of chondrule	B III							G III	G IV
Chondrule number	No. 13	No. 142	No. 12	No. 168	No. 154	No. 41	No. 300	No. 179	No. 114
SiO_2	45.24	46.41	45.10	45.00	45.55	49.61	50.58	43.14	53.08
Al_2O_3	2.09	3.09	5.86	6.89	2.19	3.62	3.19	3.25	1.42
MgO	28.20	25.12	28.20	23.82	26.91	24.52	24.04	28.73	18.78
ΣFeO	19.07	20.47	13.34	14.89	17.50	14.81	15.85	17.71	20.07
MnO	0.44	0.46	0.28	0.35		0.44	0.46	0.43	0.75
CaO	2.89	1.99	0.94	1.17	1.59	3.91	2.12	1.39	1.23
Na_2O	1.34	1.96	2.94	3.41	1.50	2.25	2.16	0.96	1.02
K_2O	0.13					0.21	0.17		0.15
Cr_2O_3	0.39		0.22			0.59			
TiO_2	0.09					0.25	0.16		0.05
NiO		0.23		0.06				1.66	0.00
Total	99.88	99.73	96.88	95.59	95.24	100.21	98.73	97.27	96.55

Group of chondrule	R IV										
Chondrule number	No. 6	No. 196	No. 136	No. 9	No. 111	No. 175	No. 1	No. 18	No. 21	No. 185	No. 39
SiO_2	53.53	52.18	52.82	52.72	52.85	53.10	55.47	55.90	54.92	56.80	56.52
Al_2O_3	2.53	2.18	2.92	2.64	2.88	2.15	2.56	3.26	1.83	3.28	1.73
MgO	25.36	20.05	26.01	27.82	24.84	21.88	25.62	25.52	30.62	23.81	25.44
ΣFeO	14.40	18.64	10.07	8.99	9.96	15.07	8.69	7.99	5.50	8.00	10.43
MnO	0.64		0.71	0.40	0.27	0.72	0.54	0.55	0.19	0.33	0.63
CaO	1.82	1.78	2.02	1.45	3.33	1.45	2.26	2.36	1.66	2.53	1.63
Na_2O	1.23	1.16	1.46	1.21	1.57	1.29	1.53	1.73	0.37	1.69	0.91
K_2O	0.02							0.03	0.03		0.05
Cr_2O_3				0.63			0.71				0.70
TiO_2	0.10							0.14	0.05		0.13
NiO			0.14		0.02	0.00				0.09	
Total	99.63	95.99	96.15	95.86	95.72	95.66	97.38	97.48	95.17	96.53	98.17

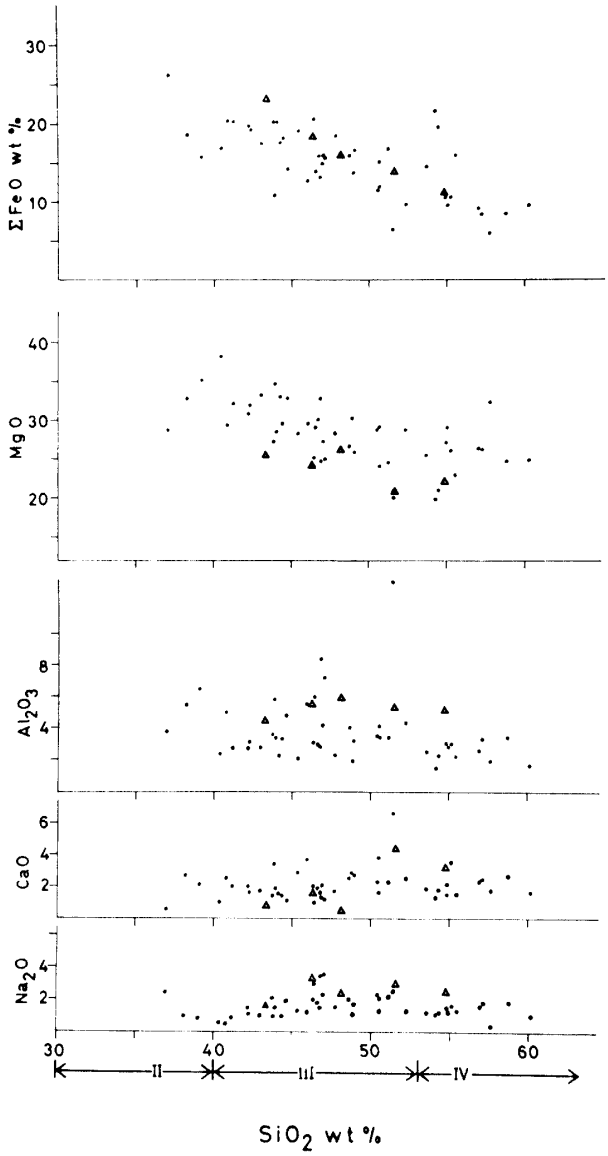

Fig. 1. Bulk chemical composition of chondrules (closed circle) and matrix (open triangle) in the Yamato-74191 meteorite. Arrows at the bottom show the range of SiO_2 contents for each class of chondrules.

include opaque minerals in considerable amounts. In these cases, Fe in opaque minerals is calculated as FeO. Therefore, the chemical composition of these chondrules may include some error in their Fe contents.

The results of chemical analyses of chondrules are shown in Table 2. The chemical composition of chondrules shows a very wide range, especially in the SiO_2 contents. The chemical composition of chondrules is plotted against normalized SiO_2 wt.% in Fig. 1, where each oxide is recalculated in such a way that the

total wt.% is normalized to 100%.

3.2. *Grouping of chondrules*

As the chondrules of Yamato-74191 show very wide range in their SiO_2 contents and their variation in texture is found to be a function of their SiO_2 contents, they are classified by their normalized SiO_2 wt.% into four classes, I, II, III and IV. Their ranges of SiO_2 contents are; I<30 wt.%, 30<II<40 wt.%, 40<III<53 wt.% and 53 wt.%<IV. The class III chondrules are further divided into two subclasses III′ and III″ at the point of 44 wt.%. The only one chondrule of class I is found in Yamato-74191 and is the metallic chondrule which includes small worm-like grains of pyroxene (Fig. 2a). The chondrules of class II have equigranular or porphyritic texture (Figs. 2b and c). Sometimes, the chondrules have a corona texture around them (Fig. 2b). The class III chondrules show porphytiric to equigranular texture (Figs. 2d and e), barred-olivine texture (Fig. 2f) or glassy (or devitrified) textures (Fig. 2g). The class IV chondrules include excentro-radial pyroxene chondrules (Fig. 2h) and glassy (or devitrified) chondrules (Fig. 2m).

Table 3. Classification of chondrules.

Texture / SiO_2 wt.%	Metallic	Porphyritic, equigranular	Barred-olivine	Glassy, devitrified	Radial-pyroxene
I<30	M I (Met+Pyx)				
30< II <40		P II (Ol+Met±Pyx)			
40< III <53		P III (Ol+Pyx±Met)	B III (Ol±Pyx)	G III (Pyx)	
53<IV				G IV	R IV (Pyx±Ol)

Met : Metallic phases or sulfide phase
Pyx : Pyroxenes
Ol : Olivine

Now on the basis of their SiO_2 contents and textures we can classify the chondrules of Yamato-74191 into seven groups, M I, P II, P III, B III, G III, G IV and R IV as shown in Table 3, where mineral assemblages characteristic to each group are listed together.

3.3. *Size of chondrules*

The apparent size of nearly round-shaped chondrules larger than about 200 μm in diameters is measured under a microscope. The mean diameter of chondrules

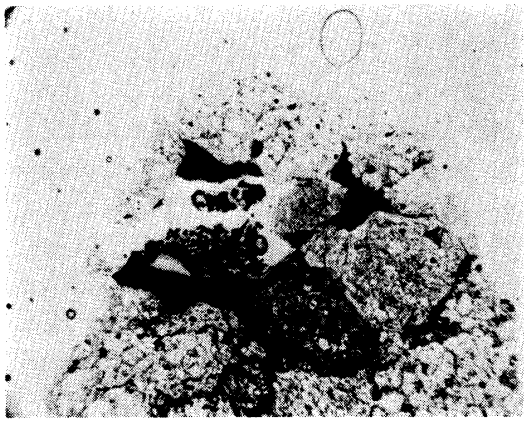

a. Central left; M I chondrule. Open nicol.

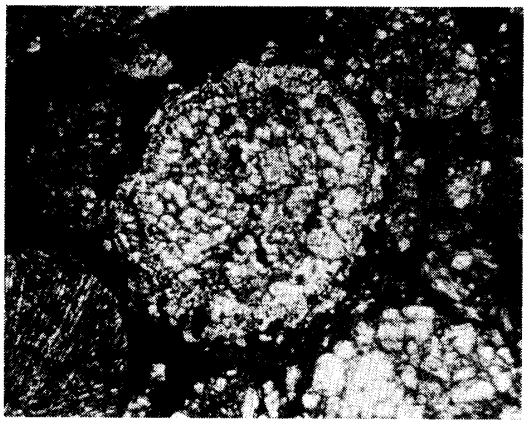

b. Central; P II chondrule having a corona texture. Open nicol.

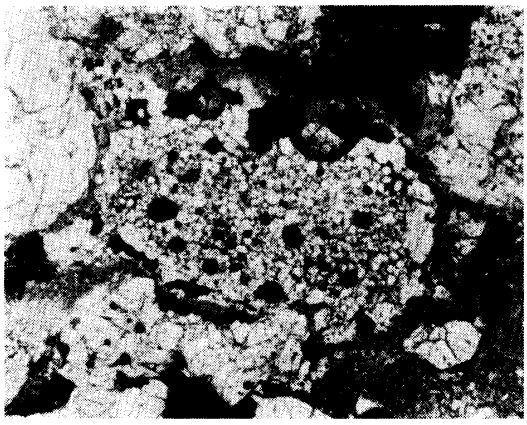

c. Central; P II chondrule. Open nicol.

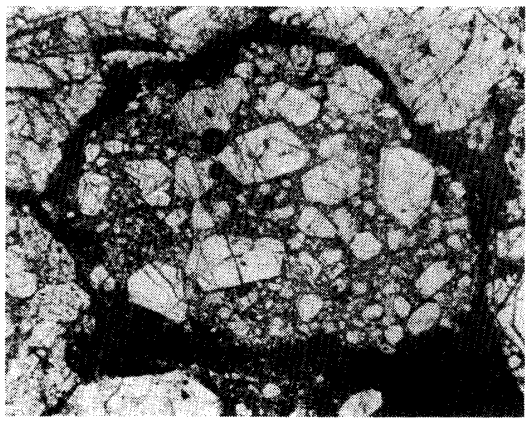

d. Central; P III′ chondrule. Open nicol.

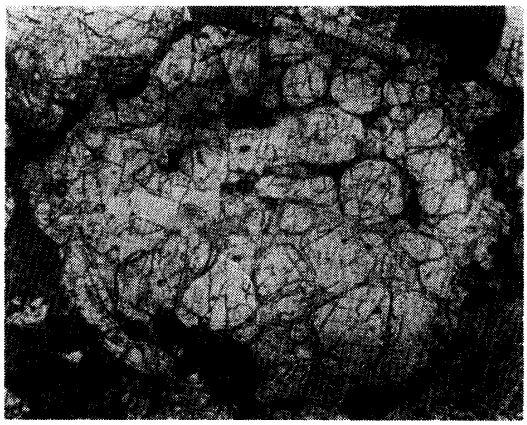

e. Central; P III′′ chondrule. Open nicol.

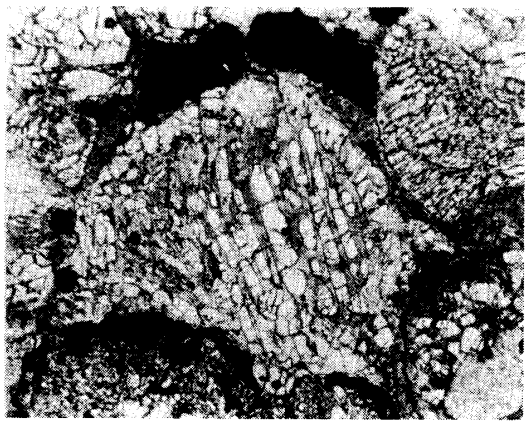

f. Central; B III chondrule. Open nicol.

Fig. 2. Photographs of chondrules, mineral fragments and matrix.

g. Central; G III chondrule. Open nicol.

h. Central; R IV chondrule. Open nicol.

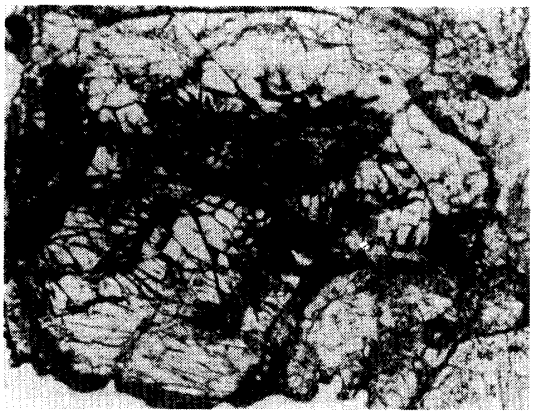

i. Central; olivine fragment. Open nicol.

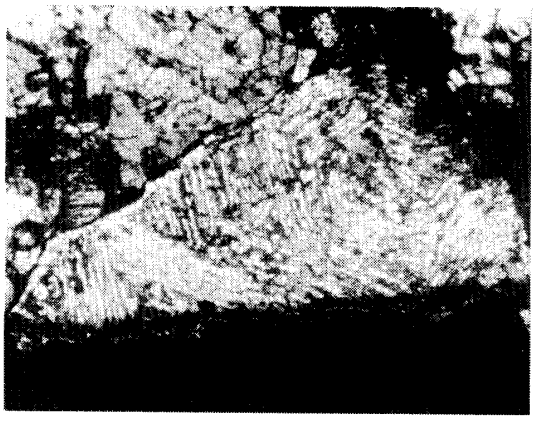

j. Central; lamellae-olivine fragment. Crossed nicols.

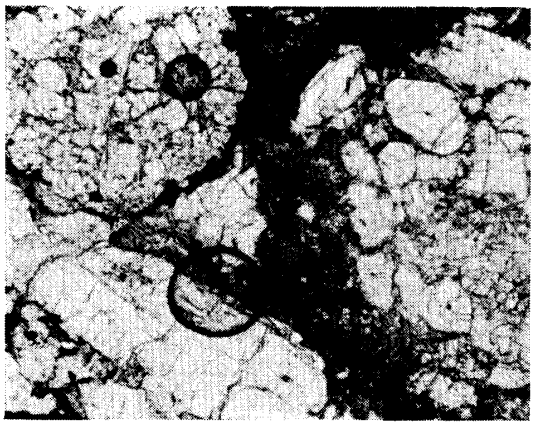

k. See text. Open nicol.

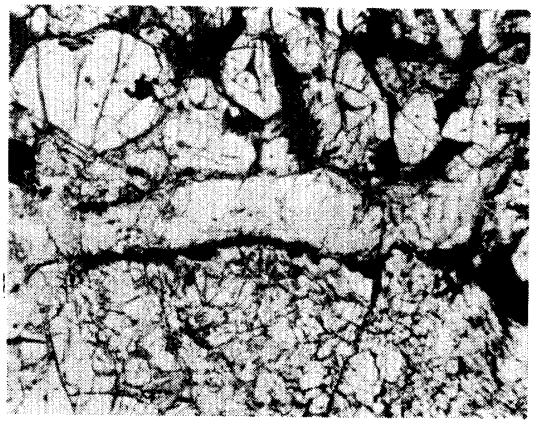

l. See text. Open nicol.

Scale: 3.2 mm × 2.6 mm for a and b, and 1 mm × 0.8 mm for the others.

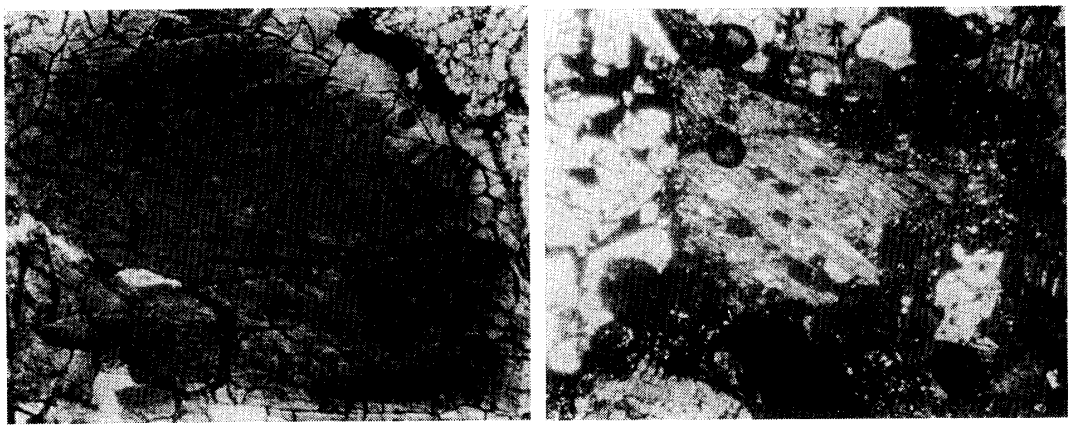

m. Central; G IV chondrule. Open nicol. *n. Central; pyroxene fragment. Crossed nicols.*

Fig. 2. Photographs of chondrules, mineral fragments and matrix. Scale: 3.2 mm×2.6 mm for a and b, and 1 mm×0.8 mm for the others.

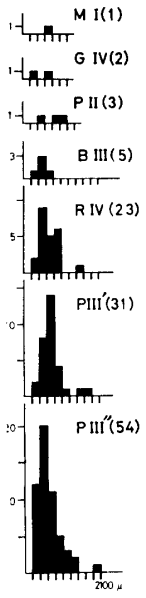

Fig. 3. Frequency diagram of apparent diameter of chondrules.

is calculated by $1/2\times$(short diameter+long diameter). The results are shown in Fig. 3, where the frequency of chondrule size of each group is shown. The size of the chondrule of the M I group is about 700 μm in apparent diameter. The chondrules of P III′, P III″, B III and R IV have peaks at about 500 μm to 700 μm, and there is no systematic change of chondrule-sizes among all groups. As nearly all round-shaped chondrules are measured in the same area of about 1 cm^2, the numbers in parentheses in Fig. 3 represent the occurrence-frequency of chondrules of each group. Therefore, the group P III is the most common type

in the meteorite and the next one is R IV. The chondrules of the groups M I, P II, G III and G IV are very rare.

4. Mineralogy

The mole ratios of SiO_2, MgO and ΣFeO of chondrules of each group are plotted in Fig. 4. The chondrules of P II and P III′ show olivine liquidus tem-

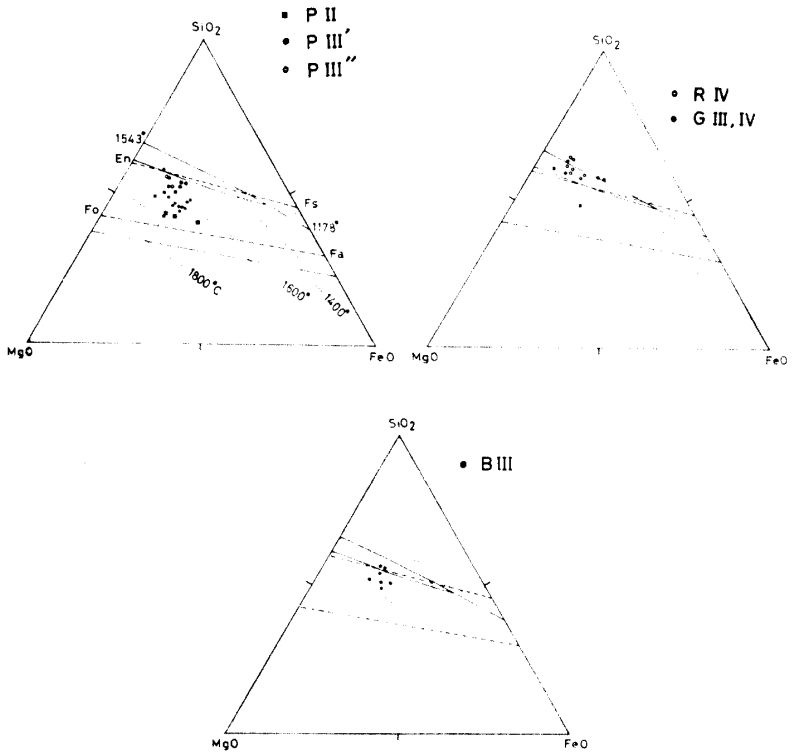

Fig. 4. The mole ratios of SiO_2, MgO and ΣFeO of chondrules of each group. Isotherms of liquidus surfaces of olivine, pyroxene and silica mineral and cotectic lines (BOWEN and SCHAIRER, 1935) are shown by dotted and solid curves, respectively. The dash curves show the solid solutions of olivine and pyroxene.

peratures of 1600° to 1800°C and those of P III″ show the temperatures of 1500° to 1600°C, although the Mg–Fe ratios of P II, P III′ and P III″ chondrules overlap each other. The chemical composition of the B III chondrules is plotted near the cotectic line of olivine and pyroxene. Although the chondrule of G III is plotted on olivine liquidus surface of about 1600°C, microphenocrystic pyroxene crystals only are observed in it. The R IV chondrules have the composition rich in SiO_2 to be plotted in pyroxene liquidus field, and their Mg–Fe ratios are almost the same as those of the other groups.

4.1. *M I chondrule*

The chondrule of M I consists of kamacite, taenite and worm-like pyroxene. The pyroxene is nearly homogeneous at about $En_{70}Wo_{1.5}$. Kamacite is the main phase in the chondrule and shows slight zoning on the Fe–Ni ratio from 3 to 6 Ni wt.%. Taenite is relatively heterogeneous around 50 Ni wt.% and might be considered from the texture to be exsolved from the host kamacite.

4.2. *P II chondrules*

The P II chondrules consist mainly of olivine, opaque minerals and groundmass. The groundmass is mainly glass. Pyroxene is rarely observed in the corona of a chondrule and not observed in the inner main part of chondrule. The chemical composition of olivines in three chondrules of this group is shown in Fig. 5d.

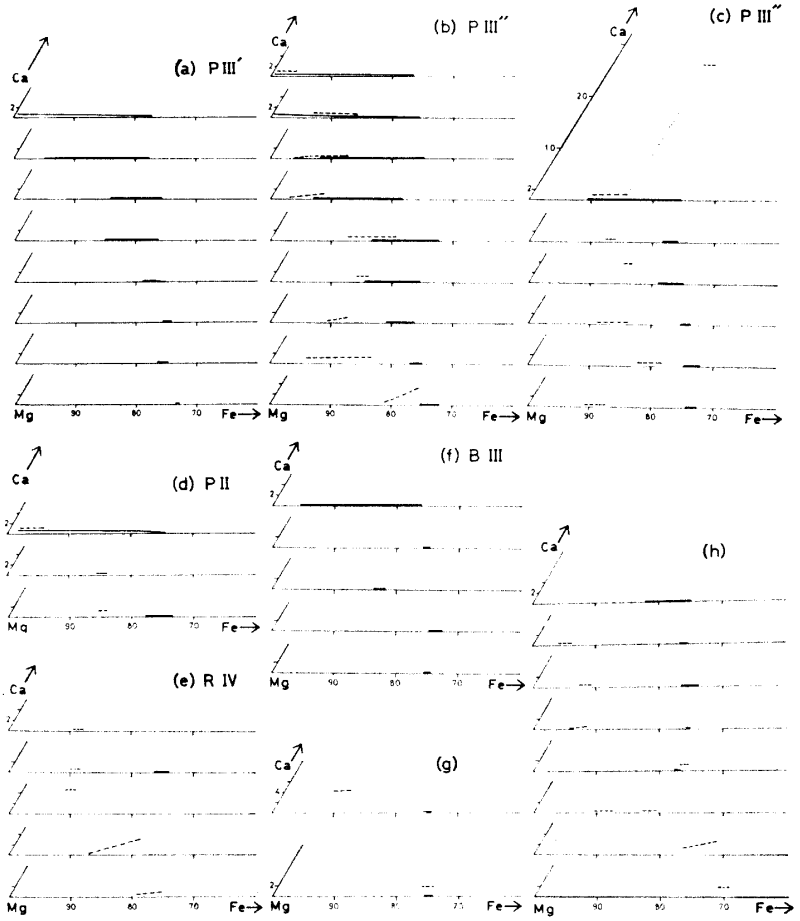

Fig. 5. The compositional ranges of olivine (solid line) and pyroxene (dash line) are shown in atomic ratios of Ca, Mg and Fe. One triangle shows the range of olivine and pyroxene in one chondrule. (g) and (h) show the ranges of lamellae-olivine fragments and the olivine and pyroxene fragments, respectively.

In the case where a chondrule shows corona texture, olivine in the inner main part is heterogeneous on the Mg–Fe ratio, although olivine in the corona is relatively homogeneous with the composition close to the most ferrous one in the chondrule. For example, the chondrule of No. 101 has a remarkable corona texture, and the olivine in the inner main part ranges from $Fo_{98}La_{0.5}$ to $Fo_{77}La_{0.0}$ (Fo and La here mean the forsterite Mg_2SiO_4 and larnite Ca_2SiO_4 molecules, respectively), whereas olivine in the corona is about $Fo_{75}La_{0.0}$. Pyroxene in the corona is relatively homogeneous ($En_{98}Wo_1$ to $En_{95}Wo_1$).

The opaque minerals in the P II chondrules are kamacite, taenite and troilite. Troilite replaces peripheral parts of taenite and kamacite grains and may be considered to be a secondary mineral. In general, two occurrences of taenite are observed. The primary taenite occurs in an isolated grain and is homogeneous at about 40 Ni wt.%. The second occurrence of taenite is observed to be included by kamacite and considered to be exsolved from the host kamacite. The exsolved taenite has heterogeneous composition of about 30 to 50 Ni wt.%, and the composition of the host kamacite is about 3 to 6 Ni wt.%.

4.3. P III′ chondrules

The P III′ chondrules consist mainly of olivine and groundmass. Chromite is observed in one chondrule of this group. The groundmass is composed of devitrified glass, (needle olivine+glass) or (unidentified small crystals+devitrified glass). The chemical composition of groundmass is measured by the same method as for those of chondrules, and the results are tabulated in Table 4. The porphyritic texture of P III′ is due to euhedral olivine phenocrysts. The chemical composition of olivines in some chondrules shows remarkable zoning from magnesian core to ferrous rim. However, olivines in some chondrules are fairly homogeneous at about the same Mg–Fe ratio as the ferrous rim of zoned olivines in the above-stated chondrules (Fig. 5a). For example, phenocrystic olivines in the No. 20 chondrule show wide zoning from $Fo_{99}La_{0.7}$ to $Fo_{77}La_{0.3}$, whereas olivines of No. 2 chondrule are homogeneous at about $Fo_{75-74}La_{0.0}$.

4.4. P III″ chondrules

The chondrules of P III″ are composed mainly of olivine, pyroxene and groundmass. Small amounts of opaque minerals are observed in one chondrule of this group. The groundmass is very clear glass in some chondrules and fine grained aggregates in the other chondrules. Their chemical compositions are shown in Table 4. The Mg–Fe zoning of olivines shows the same situation as that of the P III′ chondrules (Figs. 5b and c). The mode of pyroxene varies with their SiO_2 contents of the chondrules. When a chondrule is relatively low in SiO_2 content, a small amount of pyroxene occurs near the periphery of the chondrule. When a chondrule is rich in SiO_2, pyroxene is observed evenly in the whole area.

Pyroxenes of some chondrules show zoning from magnesian core to ferrous rim whereas those of some chondrules are homogeneous (Figs. 5b and c). In general, pyroxenes are more magnesian than olivines. Some pyroxenes include small grains of olivine. Whenever small grains of olivine are included in pyroxene crystals, they show the most ferrous composition. Therefore, the crystallization of pyroxene may occur simultaneously with or after the crystallization of the ferrous olivine.

It is to be noted that the chemical composition and zoning patterns of pyroxene have no direct relation with those of olivine. In the case of No. 11 chondrule, olivines range from $Fo_{99}La_{0.5}$ to $Fo_{76}La_{0.0}$ whereas pyroxenes range from $En_{98}Wo_1$ to $En_{96}Wo_1$ which include small grains of olivine of $Fo_{77}La_{0.0}$. In the case of No. 37 chondrule, olivine ranges from $Fo_{91}La_0$ to $Fo_{75}La_0$ and pyroxene zones from $En_{89}Wo_1$ to $En_{84}Wo_1$. This pyroxene has a very thin rim of subcalcic augite of $En_{58}Wo_{26}$. In the case of No. 26 chondrule, olivine is homogeneous at about $Fo_{76}La_0$ whereas pyroxene ranges from $En_{93}Wo_1$ to $En_{83}Wo_1$.

4.5. B III chondrules

Barred-olivine chondrules consist of olivine and groundmass which is either clear or devitrified glass. Corona texture is observed around peripheral part of some chondrules. Some chondrules of B III include small grains of pyroxene in the periphery of the chondrules. The chemical composition of the groundmass is shown in Table 4. The Mg–Fe zoning of olivine is shown in Fig. 5f. For example, olivine of No. 12 chondrule shows a distinct zoning from $Fo_{95}La_0$ at the core to $Fo_{75}La_0$ at the rim. In the case of No. 168 chondrule which has a corona texture, small pyroxene crystals are observed in the corona and their chemical composition is heterogeneous ($En_{93}Wo_1$ to $En_{83}Wo_2$), whereas olivines in the corona and the inner main part are homogeneous at $Fo_{75-74}La_0$.

4.6. G III and G IV chondrules

Only one chondrule of each group G III and G IV is observed in Yamato-74191. In the chondrule of G III (Fig. 2g), small phenocrystic pyroxenes are scattered in the devitrified glass. The composition of the pyroxenes is heterogeneous and ranges from $En_{90}Wo_0$ to $En_{75}Wo_1$. The chemical composition of the devitrified groundmass nearly equals that of the bulk chondrule (No. 179 in Table 2) because of negligible amounts of microphenocrystic pyroxene. The G IV chondrule is composed of devitrified glass and its chemical composition is tabulated in Table 2 (No. 114).

4.7. R IV chondrules

The chondrules of R IV show an excentro-radial pyroxene texture, and consist of pyroxene and groundmass. Some chondrules include small grains of olivine in radially elongated pyroxenes. The groundmass is composed mainly of

Table 4. Chemical composition of glass (gl) and groundmass (gr).

	P III″ 11-1	P III″ 11-3	P III′ 20-1	P III′ 19-4	P III′ 15-1	P III″ 28-1	P III″ 26-1	P III″ 22-12	P III″ 4-14	B III 12-2	B III 13-2	R IV 9-2	R IV 1-4
	gl	gl	gl+cx	gl+cx	gr	gl	gl	gl	gr	gl	gr	gl	gr
Na_2O	10.22	11.65	2.88	4.12	2.08	9.5	13.89	6.74	5.02	10.76	2.99	6.26	1.55
MgO	6.91	4.52	7.38	6.11	29.41	3.56	1.46	2.54	9.59	7.20	12.58	1.97	25.94
Al_2O_3	17.06	20.38	17.99	8.34	3.41	16.10	24.32	19.36	8.12	17.67	4.66	18.04	2.35
SiO_2	58.66	56.75	52.16	60.50	42.65	64.07	60.01	60.00	62.37	57.10	51.31	69.90	59.45
K_2O	0.28	0.31	0.09		0.12	0.21				0.23			0.01
CaO	2.61	1.90	13.75	10.02	2.09	2.14	0.05	7.22	9.02	3.45	5.67	3.34	1.91
TiO_2	0.54	0.54	0.48		0.13	0.49	0.67			0.05			
Cr_2O_3				0.42					0.69		0.40		
MnO	0.16	0.08	0.31	0.32	0.37	0.11	0.02	0.59	0.39	0.14	0.30	0.10	0.99
ΣFeO	3.60	2.89	2.38	8.76	18.22	2.54	1.47	1.68	6.45	3.02	10.90	0.84	8.10
Total	100.05	99.02	97.43	98.58	98.49	99.51	102.93	98.14	101.65	101.20	98.82	100.45	100.46

cx: Fine-grained crystals.

an aggregate of fine grained pyroxenes. The chemical composition of the groundmass is shown in Table 4. Radial pyroxenes of some chondrules show moderate Mg–Fe zoning although pyroxenes of the other chondrules are homogeneous (Fig. 5e). For example, in the case of No. 111 chondrule, pyroxene ranges from $En_{87}Wo_{0.2}$ to $En_{77}Wo_3$. In the case of No. 9 chondrule, pyroxene is homogeneous at about $En_{89}Wo_{0.5}$, and the euhedral olivine included in the radial pyroxene is $Fo_{74-76}La_0$.

4.8. Mineral fragments

Mineral fragments include opaque mineral fragments, pyroxene fragments, olivine fragments and lamellae-olivine fragments. Three lamallae-olivine fragments are observed in Yamato-74191. The bulk chemical composition is shown in Table 5 (Nos. 8, 10, 27 and 110). In the case of No. 8 fragment, olivine lamellae are very narrow about two or three microns in width and the host is homogeneous pyroxene. Thin olivine rims the border of the fragment. The olivine lamellae have a fixed orientation against the pyroxene host as shown in Fig. 2j. The compositions of olivine and pyroxene are about $Fo_{74-76}La_{0-0.5}$ and $En_{85-87}Wo_{4-5}$, respectively (Fig. 5g). The volume ratio of lamellae olivine to the host pyroxene is about 1/2 or 1/3.

Pyroxene fragments are homogeneous to moderately zoned on Mg–Fe (Fig. 5h). Some of the pyroxene fragments include small grains of olivine. In the case of No. 7 fragment, pyroxene of $En_{94}Wo_{0.3}$ to $En_{91}Wo_{0.5}$ includes small crystals of olivine of $Fo_{76}La_0$ to $Fo_{74}La_0$.

Olivine fragments are also homogeneous to moderately zoned on Mg–Fe (Fig. 5h). Some grains of olivine include small crystals of pyroxene. For

Table 5. Bulk chemical composition of silicate fragments of the Yamato-74191 meteorite.

	No. 8	No. 10	No. 27	No. 110
SiO_2	47.85	50.26	54.09	49.79
Al_2O_3	2.45	3.06	2.18	3.75
MgO	31.79	25.47	21.83	29.32
ΣFeO	10.11	17.18	16.29	9.85
MnO	0.22	0.45	0.72	0.36
CaO	2.94	2.26	1.51	2.56
Na_2O	0.25	1.73	1.29	0.34
K_2O	0.01	0.14	0.02	
TiO_2	0.12	0.11	0.07	
NiO				0.10
Total	95.74	100.66	98.01	96.08

example, olivine of No. 23 (Fig. 2i) includes several small grains of pyroxene, and both the host olivine and included pyroxene are homogeneous. The chemical compositions of pairs of olivine and pyroxene in contact with each other are ($Fo_{77.7}La_{0.0}$ and $En_{76.0}Wo_{0.8}$), ($Fo_{76.8}La_{0.0}$ and $En_{75.7}Wo_{1.3}$) and ($Fo_{76.8}La_{0.0}$ and $En_{75.3}Wo_{1.2}$).

Opaque minerals of the opaque mineral fragments are kamacite, taenite and troilite. Opaque mineral fragments show irregular-shapes and sometimes interstitial-filling texture between chondrules. Troilite occurs usually in the periphery of or along cracks in kamacite or taenite fragments. Therefore, troilite seems to be a secondary mineral which replaced kamacite or taenite after the formation of the meteorite. Some kamacite fragments are free from inclusions of taenite and some include minute crystals of taenite which might have been exsolved from the host kamacite. The chemical composition of kamacite and the exsolved taenite are about 3 to 6 Ni wt.% and 30 to 50 Ni wt.%, respectively. Some taenite fragments are free from inclusions and the others include small grains of kamacite which seem to be exsolved from the host taenite. The composition of taenite is heterogeneous and ranges from 35 to 50 Ni wt.%.

5. Matrix

The chemical composition of the matrix of Yamato-74191 is measured by the same method as that of chondrules. The results of analyses are shown in Table 6 and plotted in Fig. 1. As shown in the figure, the composition of the matrix has nearly the same trend as that of chondrules except the tendency of low MgO and high Na_2O and Al_2O_3.

Fig. 2*l* shows a mineral fragment of olivine between two chondrules. Some

Table 6. Chemical composition of matrix.

	26-12	16-1	16-2	17-2
Na_2O	2.32	3.15	2.36	3.03
MgO	25.23	23.07	21.16	20.84
Al_2O_3	5.67	5.53	5.03	5.28
SiO_2	46.33	44.68	52.75	51.83
K_2O		0.16	0.33	0.39
CaO	0.45	1.54	3.10	4.38
TiO_2		0.10	0.12	0.19
Cr_2O_3	0.56			
MnO	0.35	0.32	0.44	0.39
ΣFeO	15.42	17.84	10.70	14.06
Total	96.33	96.18	96.00	100.40

parts of the olivine tend to become an aggregate of very fine-grained olivine which shows wavy extinction under a microscope, and some parts are relic homogeneous olivine whose composition is $Fo_{74.8}La_{0.0}$. The chondrule shown in the right side of Fig. 2k seems to be ground off to be separated from the left part of the chondrule by the fine-grained matrix zone shown in the central part of the figure. These observations show that some parts of the matrix were formed by fragmentation or grinding of chondrules or mineral fragments.

6. Mg–Fe Compositional Relation between Chondrules and Minerals in Them

The Mg–Fe zoning of olivine and pyroxene varies from chondrule to chondrule even within the same group. Some chondrules include both large olivine crystals showing distinct zoning and small olivine crystals being relatively homogeneous. On the other hand, some chondrules include large and small homogeneous crystals of olivine. Figs. 6a and c show an intimate compositional relation between P III chondrules and olivines in them. Namely, (1) the magnesian chondrules of P III contain olivine crystals which show a wide compositional range

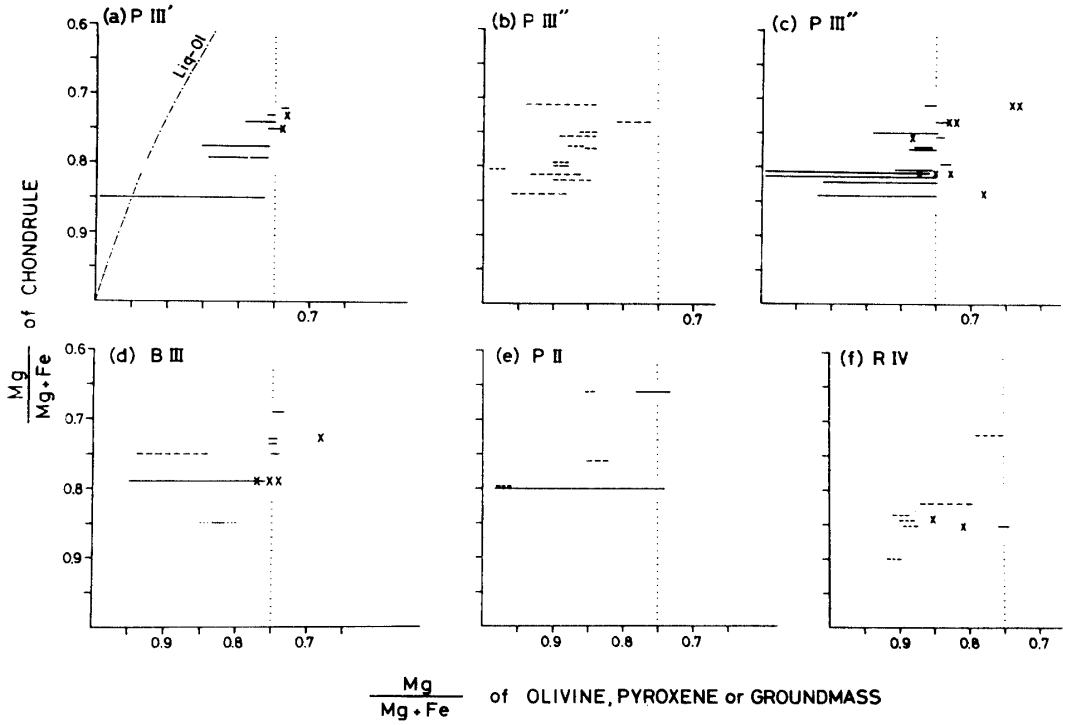

Fig. 6. The compositional ranges of olivine (solid line), pyroxene (dash line) and groundmass (cross) in chondrules, are shown against Mg/(Mg+Fe) atomic ratios of their host chondrules. The dot-dash curve: see text.

from extremely magnesian olivine to ferrous one, whereas olivine crystals in the ferrous chondrules of P III are homogeneous. (2) The ferrous olivines in both magnesian and ferrous chondrules of P III have nearly the same composition of $Fo_{75\pm2}$. (3) The chemical composition of pyroxenes of P III'' chondrules, however, does not show an intimate correlation with the composition of their host chondrules (Fig. 6b). (4) The Mg/(Mg+Fe) ratios of the groundmass in most P III chondrules are within the range of 0.73 ± 0.10.

The compositional ranges of olivine and/or pyroxene of three P II chondrules are shown in Fig. 6e. As the P II chondrules include opaque minerals in relatively large amounts, the vertical axis of (e) in Fig. 6 means $Mg^{2+}/(Mg^{2+}+Fe^{2+}+Fe^{0})$, Fe^{0} here means Fe in opaque minerals and partially in groundmass. Taking abundant occurrence of opaque minerals in the P II chondrules into account, the same situation of compositional relations as the P II chondrules is observed.

In the B III chondrules, the nearly same compositional relations as P III are recognized.

The compositional relations between the R IV chondrules and olivines cannot be obtained as olivines rarely occur in R IV chondrules. However, (5) pyroxenes in the magnesian R IV chondrules are more magnesian and those in the ferrous R IV chondrules are more ferrous.

The above-stated compositional relations (1) to (5) may be important in considering the origin of chondrules. The other important criteria on the origin of chondrules are (6) later crystallization of extremely or moderately magnesian pyroxene after the crystallization of ferrous olivine already discussed in the Section 4, and (7) the rapid cooling rate of chondrules which will be discussed in the next section.

7. Cooling Rate of Chondrules

The chemical composition of clean glass in some chondrules is tabulated in Table 4. Their normative mode consists mainly of albite and pyroxene with minor amounts of nepheline or quartz and/or olivine if all Fe in those glass is assumed as FeO. If a chondrule crystallized slowly, the glass could not be formed in the chondrule and the interstitial melt changed into crystal aggregate mainly of sodic plagioclase with various amounts of pyroxene.

The average grain size (W in microns) of plagioclase crystallizing from silicate melt will be controlled by the following equation (IKEDA, 1977);

$$W=1/3 \log t+ \log 2\eta^{-1/3}$$

where t is time in seconds necessary for plagioclase of grain size W to crystallize at nearly constant temperature and η is viscosity of the melt in poise. As the viscosity of a silicate melt can be calculated by the method of BOTTINGA and

WEILL (1972), the time necessary for plagioclase of about 1 micron in average width to grow from the melt at each temperature can be obtained and is shown in Table 7. The existence of clean glass in some chondrules of Yamato-74191 suggests at least that the cooling rate of those chondrules is more rapid than those inferred from the values of Table 7. For example, in the case of No. 11 chondrule which belongs to the P III group, the time necessary for cooling from the temperature at the

Table 7. Crystallization time in seconds necessary for the glass in various chondrules to crystallize into plagioclase of about 1 micron in average width.

	P III (11-1)	P III (11-2)	P III (28-1)	P III (26-1)	B III (12-2)	B III (12-1)	R IV (9-2)
1000°C	1.5×10^{4}	2.0×10^{4}	0.4×10^{5}	0.6×10^{5}	8.3×10^{3}	1.5×10^{4}	2.5×10^{5}
800°C	0.7×10^{6}	0.8×10^{6}	1.7×10^{6}	2.5×10^{6}	0.3×10^{6}	5.5×10^{5}	0.9×10^{7}
600°C	1.4×10^{8}	1.1×10^{8}	0.3×10^{9}	4.5×10^{8}	0.5×10^{8}	8.3×10^{7}	1.3×10^{9}
400°C	1.0×10^{12}	0.6×10^{12}	1.3×10^{12}	3.5×10^{12}	1.4×10^{11}	0.3×10^{12}	0.5×10^{13}
200°C	1.5×10^{19}	2.0×10^{18}	5.5×10^{18}	1.4×10^{19}	2.5×10^{17}	1.0×10^{18}	1.4×10^{19}

formation of the interstitial melt to about 800° or 400°C, cannot be larger than 0.7 to 0.8×10^{6} seconds (about 8 days) or 0.6 to 1.0×10^{12} seconds (several tens thousands years), respectively. The values shown in Table 7 indicate that most chondrules of Yamato-74191 experienced rapid cooling at the high temperature range, and that the meteorite has not been heated for a long time at temperatures higher than at least 400°C since its formation.

8. Discussion

The above-stated relations (1) to (7) set the severe constraints upon the origin and crystallization of chondrules.

The fractional crystallization of a silicate melt drop in the closed system cannot fully explain the compositional relations. The partition coefficient of Mg and Fe between olivine and silicate melt ($K_D=x_{Fe}^{Ol}x_{Mg}^{Melt}/x_{Mg}^{Ol}x_{Fe}^{Melt}$) is about 0.3 for high temperature range (ROEDER and EMSLIE, 1970). The Mg–Fe ratios of the olivine, which must crystallize firstly in silicate melt drops of various Mg–Fe ratios in the closed system, are calculated using the K_D value of 0.3, and shown in Fig. 6a by dot-dash curve denoted as Liq-Ol. It is clearly indicated by the figure that the Mg–Fe ratios of the most magnesian and ferrous olivines in the P III chondrules cannot be explained by fractional crystallization in the closed system. The partition coefficient between olivine and pyroxene at high temperature range given by LARIMER (1968) cannot also explain the extremely magnesian composition of pyroxene which crystallized after the precipitation of ferrous olivine of about 0.75 Mg–Fe ratio.

The fractional crystallization in a closed system cannot explain also the compositional relation (2).

BLANDER and ABDEL-GAWAD (1969) explained the ferrous nature of olivine coexisting with magnesian pyroxene by diffusion process which took place after the crystallization of chondrules including only magnesian olivine and pyroxene. However, their model does not fit the relation (4) for the following reason. If their model is the case, the Mg–Fe ratios of interstitial glass coexisting with ferrous olivine must have values lower than those reported in this paper, because the thorough diffusion of Mg–Fe to the interstitial glass should take place as well as in olivine crystals and the interstitial glass should be nearly in equilibrium with the ferrous olivine in contact with the glass.

In conclusion, we propose for the crystallization of silicate melt drops in an open system.

Primarily the formational condition of a silicate melt drop was extremely reduced one (low f_{O_2}) and the extremely magnesian olivine crystallized for the magnesian chondrules. The oxidation state of the silicate melt drop was gradually changed from low f_{O_2} to high f_{O_2} during the crystallization of olivine crystals, and ferrous olivine precipitated in the high f_{O_2} environment for the magnesian and ferrous chondrules. Next the sudden change of the oxidation state took place to low f_{O_2} again, and magnesian pyroxenes crystallized from the interstitial melt including sometimes the ferrous olivine grains.

Acknowledgments

We thank Dr. A. ONO of the National Institute for Researches in Inorganic Materials in Japan for allowing the use of the electron-probe microanalyzer, and Dr. H. SHIMAZAKI and Mr. H. HARAMURA of Geological Institute, University of Tokyo for critical reading of the manuscript and chemical analysis of the meteorite, respectively.

References

BENCE, A. E. and ALBEE, A. L. (1968): Empirical correction factors for the electron microanalysis of silicates and oxides. J. Geol., **76**, 382–403.

BLANDER, M. and ABDEL-GAWAD, M. (1969): The origin of meteorites and the constrained equilibrium condensation theory. Geochim. Cosmochim. Acta, **33**, 701–716.

BOTTINGA, Y. and WEILL, D. F. (1972): The viscosity of magmatic silicate liquids: A model for calculation. Am. J. Sci., **272**, 438–475.

BOWEN, N. L. and SCHAIRER, J. F. (1935): The system MgO–FeO–SiO_2. Am. J. Sci., **29**, 151–217.

IKEDA, Y. (1977): Grain size of plagioclase of the basaltic andesite dikes, central Abukuma plateau. Can. J. Earth Sci., **14**, 1860–1866.

LARIMER, J. W. (1968): Experimental studies on the system Fe–MgO–SiO_2–O_2 and their bearing

on the petrology of chondritic meteorites. Geochim. Cosmochim. Acta, **32**, 1187–1207.

NAKAMURA, Y. and KUSHIRO, I. (1970): Compositional relations of coexisting orthopyroxene, pigeonite and augite in a tholeiitic andesite from Hakone volcano. Contrib. Mineral. Petrol., **26**, 265–275.

ROEDER, P. L. and EMSLIE, R. F. (1970): Olivine-liquid equilibrium. Contrib. Mineral. Petrol., **29**, 275–289.

SWEATMAN, T. R. and LONG, J. V. P. (1969): Quantitative electron-probe microanalysis of rock forming minerals. J. Petrol., **10**, 332–379.

VAN SCHMUS, W. R. (1969): The mineralogy and petrology of chondritic meteorites. Earth Sci. Rev., **5**, 145–184.

VAN SCHMUS, W. R. and WOOD, J. A. (1967): A chemical-petrologic classification for the chondritic meteorites. Geochim. Cosmochim. Acta, **31**, 747–765.

WALTER, L. S. (1969): The major-element composition of individual chondrules of the Bjurböle meteorite. Symposium on Meteorite Research, ed. by P. M. MILLMAN. Dordrecht, D. Reidel, 191–205.

WOOD, J. A. (1968): Meteorites and Origin of Planets. New York, McGraw-Hill.

YANAI, K., MIYAMOTO, M. and TAKEDA, T. (1978): A classification for the Yamato-74 chondrites based on the chemical compositions of their olivines and pyroxenes. Mem. Natl Inst. Polar Res., Spec. Issue, **8**, 110–120.

(Received June 6, 1978)